Optical array generator based on blue phase liquid crystal Dammann grating

Shi-Jun Ge,[1] Peng Chen,[1] Ling-Ling Ma,[1] Zhen Liu,[2] Zhi-Gang Zheng,[2] Dong Shen,[2] Wei Hu,[1,*] and Yan-Qing Lu[1]

[1]*National Laboratory of Solid State Microstructures, Collaborative Innovation Center of Advanced Microstructures and College of Engineering and Applied Sciences, Nanjing University, Nanjing 210093, China*
[2]*Department of Physics, East China University of Science and Technology, Shanghai 200237, China*
[*] *huwei@nju.edu.cn*

Abstract: Blue phase liquid crystal Dammann grating is demonstrated as an optical array generator. The phase profile is formed by the alternation of isotropic refractive index and vertical field induced ordinary index. Periodical Dammann grating can generate equal energy distributed optical array. When forked dislocations are introduced, multiple optical vortex beams with different topological charges are generated. This approach supplies a novel design for fast-response optical array generator, which has great potentials in array illumination, beam shaping and optical communications.

OCIS codes: (230.3720) Liquid-crystal devices; (050.0050) Diffraction and gratings; (050.4865) Optical vortices.

References and links

1. N. Streibl, "Beam shaping with optical array generators," J. Mod. Opt. **36**(12), 1559–1573 (1989).
2. L. P. Boivin, "Multiple imaging using various types of simple phase gratings," Appl. Opt. **11**(8), 1782–1792 (1972).
3. W. B. Veldkamp, J. R. Leger, and G. J. Swanson, "Coherent summation of laser beams using binary phase gratings," Opt. Lett. **11**(5), 303–305 (1986).
4. H. Dammann and E. Klotz, "Coherent optical generation and inspection of 2-dimensional periodic structures," Opt. Acta (Lond.) **24**(4), 505–515 (1977).
5. G. Gibson, J. Courtial, M. Padgett, M. Vasnetsov, V. Pas'ko, S. Barnett, and S. Franke-Arnold, "Free-space information transfer using light beams carrying orbital angular momentum," Opt. Express **12**(22), 5448–5456 (2004).
6. J. Wang, J. Y. Yang, I. M. Fazal, N. Ahmed, Y. Yan, H. Huang, Y. Ren, Y. Yue, S. Dolinar, M. Tur, and A. E. Willner, "Terabit free-space data transmission employing orbital angular momentum multiplexing," Nat. Photonics **6**(7), 488–496 (2012).
7. T. Lei, M. Zhang, Y. Li, P. Jia, G. N. Liu, X. Xu, Z. Li, C. Min, J. Lin, C. Yu, H. Niu, and X. C. Yuan, "Massive individual orbital angular momentum channels for multiplexing enabled by Dammann gratings," Light Sci. Appl. **4**(3), e257 (2015).
8. B. Y. Wei, W. Hu, Y. Ming, F. Xu, S. Rubin, J. G. Wang, V. Chigrinov, and Y. Q. Lu, "Generating switchable and reconfigurable optical vortices via photopatterning of liquid crystals," Adv. Mater. **26**(10), 1590–1595 (2014).
9. P. Chen, B. Y. Wei, W. Ji, S. J. Ge, W. Hu, F. Xu, V. Chigrinov, and Y. Q. Lu, "Arbitrary and reconfigurable optical vortex generation: a high-efficiency technique using director-varying liquid crystal fork gratings," Photonics Res. **3**(4), 133 (2015).
10. I. Moreno, J. A. Davis, D. M. Cottrell, N. Zhang, and X. C. Yuan, "Encoding generalized phase functions on Dammann gratings," Opt. Lett. **35**(10), 1536–1538 (2010).
11. N. Zhang, X. C. Yuan, and R. E. Burge, "Extending the detection range of optical vortices by Dammann vortex gratings," Opt. Lett. **35**(20), 3495–3497 (2010).
12. Z. Wang, N. Zhang, and X. C. Yuan, "High-volume optical vortex multiplexing and de-multiplexing for free-space optical communication," Opt. Express **19**(2), 482–492 (2011).
13. J. Yu, C. Zhou, W. Jia, J. Wu, L. Zhu, Y. Lu, C. Xiang, and S. Li, "Generation of controllable rotating petal-like modes using composited Dammann vortex gratings," Appl. Opt. **54**(7), 1667–1672 (2015).
14. Y. Chen, J. Yan, J. Sun, S. T. Wu, X. Liang, S. H. Liu, P. J. Hsieh, K. L. Cheng, and J. W. Shiu, "A microsecond-response polymer-stabilized blue phase liquid crystal," Appl. Phys. Lett. **99**(20), 201105 (2011).

#258583 Received 1 Feb 2016; revised 7 Mar 2016; accepted 7 Mar 2016; published 9 Mar 2016

15. S. C. Chen, P. C. Wu, and W. Lee, "Dielectric and phase behaviors of blue-phase liquid crystals," Opt. Mater. Express **4**(11), 2392–2400 (2014).
16. D. Xu, J. Yan, J. Yuan, F. Peng, Y. Chen, and S. T. Wu, "Electro-optic response of polymer-stabilized blue phase liquid crystals," Appl. Phys. Lett. **105**(1), 011119 (2014).
17. Z. Ge, S. Gauza, M. Jiao, H. Xianyu, and S. T. Wu, "Electro-optics of polymer-stabilized blue phase liquid crystal displays," Appl. Phys. Lett. **94**(10), 101104 (2009).
18. L. Rao, Z. Ge, S. Gauza, K. M. Chen, and S. T. Wu, "Emerging liquid crystal displays based on the Kerr effect," Mol. Cryst. Liq. Cryst. (Phila. Pa.) **527**(1), 30–42 (2010).
19. Y. Liu, Y. Lan, Q. Hong, and S. T. Wu, "Compensation film designs for high contrast wide-view blue phase liquid crystal displays," J. Disp. Technol. **10**(1), 3–6 (2014).
20. Y. H. Lin, H. S. Chen, H. C. Lin, Y. S. Tsou, H. K. Hsu, and W. Y. Li, "Polarizer-free and fast response microlens arrays using polymer-stabilized blue phase liquid crystals," Appl. Phys. Lett. **96**(11), 113505 (2010).
21. Y. Li and S. T. Wu, "Polarization independent adaptive microlens with a blue-phase liquid crystal," Opt. Express **19**(9), 8045–8050 (2011).
22. J. L. Zhu, J. G. Lu, J. Qiang, E. W. Zhong, Z. C. Ye, Z. He, X. Guo, C. Y. Dong, Y. Su, and H. P. D. Shieh, "1D/2D switchable grating based on field-induced polymer stabilized blue phase liquid crystal," J. Appl. Phys. **111**(3), 033101 (2012).
23. Y. T. Lin, H. C. Jau, and T. H. Lin, "Polarization-independent rapidly responding phase grating based on hybrid blue phase liquid crystal," J. Appl. Phys. **113**(6), 063103 (2013).
24. S. J. Ge, W. Ji, G. X. Cui, B. Y. Wei, W. Hu, and Y. Q. Lu, "Fast switchable optical vortex generator based on blue phase liquid crystal fork grating," Opt. Mater. Express **4**(12), 2535–2541 (2014).
25. D. Xu, G. Tan, and S. T. Wu, "Large-angle and high-efficiency tunable phase grating using fringe field switching liquid crystal," Opt. Express **23**(9), 12274–12285 (2015).
26. J. Yan, Y. Xing, and Q. Li, "Dual-period tunable phase grating using polymer stabilized blue phase liquid crystal," Opt. Lett. **40**(19), 4520–4523 (2015).
27. D. Luo, H. T. Dai, and X. W. Sun, "Polarization-independent electrically tunable/switchable Airy beam based on polymer-stabilized blue phase liquid crystal," Opt. Express **21**(25), 31318–31323 (2013).
28. J. Yu, C. Zhou, W. Jia, A. Hu, W. Cao, J. Wu, and S. Wang, "Three-dimensional Dammann vortex array with tunable topological charge," Appl. Opt. **51**(13), 2485–2490 (2012).
29. C. Zhou and L. Liu, "Numerical study of dammann array illuminators," Appl. Opt. **34**(26), 5961–5969 (1995).
30. H. Wu, W. Hu, H. C. Hu, X. W. Lin, G. Zhu, J. W. Choi, V. Chigrinov, and Y. Q. Lu, "Arbitrary photo-patterning in liquid crystal alignments using DMD based lithography system," Opt. Express **20**(15), 16684–16689 (2012).
31. W. Duan, P. Chen, B. Y. Wei, S. J. Ge, X. Liang, W. Hu, and Y. Q. Lu, "Fast-response and high-efficiency optical switch based on dual-frequency liquid crystal polarization grating," Opt. Mater. Express **6**(2), 597–602 (2016).
32. H. Kikuchi, M. Yokota, Y. Hisakado, H. Yang, and T. Kajiyama, "Polymer-stabilized liquid crystal blue phases," Nat. Mater. **1**(1), 64–68 (2002).
33. J. Yan and S. T. Wu, "Polymer-stabilized blue phase liquid crystals: a tutorial [Invited]," Opt. Mater. Express **1**(8), 1527–1535 (2011).
34. G. Zhu, J. N. Li, X. W. Lin, H. F. Wang, W. Hu, Z. G. Zheng, H. Q. Cui, D. Shen, and Y. Q. Lu, "Polarization-independent blue phase liquid crystal gratings driven by vertical electric field," J. Soc. Inf. Disp. **20**(6), 341–346 (2012).
35. J. Yan, H. C. Cheng, S. Gauza, Y. Li, M. Jiao, L. Rao, and S. T. Wu, "Extended Kerr effect of polymer-stabilized blue-phase liquid crystals," Appl. Phys. Lett. **96**(7), 071105 (2010).

1. Introduction

An optical array generator is such a device that splits an incoming laser beam into an array of many 'beamlets' [1]. It has attracted much attention due to its extensive applications in optical data storage [1], multiple imaging [2] and coherent summation of laser beams [3]. Among the wide variety of optical array generators, the so-called Dammann grating (DG) [4] is a key approach to uniformly distribute energies among the designed diffraction orders without changing its mode. In optical communications, mode based multiplexing technology can drastically enhance the capacity. Recently, orbital angular momentum (OAM) of optical vortices (OVs) has been intensively studied as it can provide a new degree of freedom for mode multiplexing [5–7]. By introducing the concept of DG into conventional vortex grating [5, 8, 9], Dammann vortex grating (DVG) can generate multiple OVs with different OAM and equal energy [7, 10]. In addition, the DVG can extend the detection capacity in OAM parallel detection as all the designed diffraction orders become useful [11].

The DGs and DVGs can be achieved via different strategies. Previously reported DGs were mainly fabricated on photoresists [7, 11, 12] or glass substrates [13] via microelectronic-

#258583 Received 1 Feb 2016; revised 7 Mar 2016; accepted 7 Mar 2016; published 9 Mar 2016

lithography. However, they are static without tunability. The commercial spatial light modulator (SLM) provides an approach to realize tunable DGs [10]. But the SLM suffers from polarization dependency, high cost and optical inefficiency. Liquid crystals (LCs) have been employed to accomplish tunable phase modulation thanks to their excellent electro-optical (EO) properties. Compared to nematic LCs, the Kerr effect of blue phase liquid crystals (BPLCs) permits fast EO response [14–16]. BPLCs have great potentials in both display [17–19] and non-display fields, such as lenses [20, 21], gratings [22–26] and cubic phase plates [27]. Therefore, the realization of BPLC DGs/DVGs make it possible for tunable, low cost and fast switchable optical array generators.

In this work, the first BPLC DGs/DVGs are demonstrated. Specific periodical and forked electrodes are utilized to drive BPLC to form DGs and DVGs, respectively. They are demonstrated as optical array generators for equal-energy distribution. For BPLC DVGs, a series of OV beams with different topological charges are generated. Besides, advantages such as fast electrical switchability and polarization independence are exhibited.

2. Principle and experiment

A DG can be obtained by binarizaing a blazed phase distribution ($\varphi = 2\pi x/\Lambda$, Λ is the period) into 0 and π phase values. The transmission function of DG can be written as [28],

$$T_{DG}(x) = \sum_{n=-\infty}^{\infty} C_n \exp(\mathrm{i}\, n \frac{2\pi}{\Lambda} x), \tag{1}$$

where n represents the diffraction order. When the vortex phase of $m\theta$ (θ is the azimuthal angle, m is the topological charge) is nested, the blazed spiral phase distribution can be depicted as $\varphi = 2\pi x/\Lambda + m\theta$. After binarization, a DVG could be obtained. Its transmission function can be written as [28],

$$T_{DG}(x,\theta) = \sum_{n=-\infty}^{\infty} C_n \exp\left[\mathrm{i}\, n(\frac{2\pi}{\Lambda} x + m\theta)\right]. \tag{2}$$

For both cases, the coefficient of the n^{th} order can be expressed as

$$C_n = \begin{cases} \dfrac{-\mathrm{i}\Lambda}{2n\pi}\left[1 + 2\sum_{k=1}^{N-1}(-1)^k \exp(-\mathrm{i}2\pi n x_k) + (-1)^N \exp(-\mathrm{i}2\pi n x_N)\right] & n \neq 0 \\ \Lambda\left[2\sum_{k=1}^{N-1}(-1)^k x_k + (-1)^N x_N\right] & n=0 \end{cases}, \tag{3}$$

where $\{x_k\}$ are normalized phase transition points in one period with boundary values of $x_0 = 0$ and $x_N = 1$, and N is the total number of transition points. By optimizing the values of $\{x_k\}$, the light energy can be distributed into several desired orders with good uniformity and high efficiency, which is the essence of Dammann phase-encoding method [28]. Zhou and Liu have reported a series of normalized phase transition points required for different number of equal-energy diffracted orders [29].

Here, DG and DVG with seven desired diffraction orders are presented using Dammann parameters $x_1 = 0.23191$, $x_2 = 0.42520$, and $x_3 = 0.52571$ [29]. The phase patterns of designed DG and DVG are shown in Figs. 1(a) and 1(e) with black indicating 0 and white indicating π. We transfer these patterns to the positive photoresist by means of Digital Micro-mirror Device (DMD) based microlithography [30, 31]. The white regions in Figs. 1(a) and (e) are exposed areas. After developing, the ITO layer corresponding to white regions is removed by wet etching. The unexposed regions, *i.e.* the black regions, still have ITO layer. Figures 1(b) and 1(f) show the obtained patterned electrodes with the period of 125 μm observed in reflection mode and the brighter regions are ITO covered regions. Then each patterned ITO glass is assembled with a bare ITO glass to form a cell. The cell gap is 12 μm controlled by

#258583 Received 1 Feb 2016; revised 7 Mar 2016; accepted 7 Mar 2016; published 9 Mar 2016

Mylar films. As aligning process is not needed for BPLC, the fabrication procedure is simplified.

The mixture of BPLC precursor contains LC host TEB300 (80.9 wt%), monomers RM257 (10 wt%) and EHA (5 wt%), chiral dopant R5011 (3.6 wt%) and photo initiator (0.5 wt%). The mixture is stirred above the clearing point and filled into the cell. We first heat the cell to 45 °C and then cool it at a rate of 0.1 °C/min. A heating and cooling stage (Linkam SLT 120) is used to precisely control the temperature and the sample is observed under a polarizing microscope (Nikon 50i) with orthogonal polarizers. A uniform BP state is obtained at 35 °C which is then UV-cured at an intensity of 3 mW/cm^2 for 5 minutes. After that, polymer-stabilized BPLC [32, 33] cells with patterned electrodes are achieved.

The BPLC is optical isotropic and the refractive index is n_i with no electric field applied. When external field is applied, the refractive index to normally incident light in the electrode covered regions changes gradually from n_i to n_o due to Kerr effect while that in the uncovered regions almost keeps n_i [34]. Here the Kerr constant is positive. According to the extended Kerr effect, the induced birefringence Δn can be characterized as [35]:

$$\Delta n(E) = \Delta n_{sat}\left(1-\exp\left[-\left(\frac{E}{E_S}\right)^2\right]\right), \tag{4}$$

$$n_o(E) = n_i - \frac{\Delta n(E)}{3}, \tag{5}$$

where Δn_{sat} is the saturated induced birefringence, E_s is the saturation electric field, and $n_o(E)$ is the field induced ordinary refractive index. In this case, the phase difference Γ between the two regions could be expressed as [35]

$$\Gamma = \frac{2\pi}{\lambda}[n_i - n_o(E)]d, \tag{6}$$

where λ is the wavelength of incident light. Thus a DG or DVG phase profile is formed.

3. Results and discussions

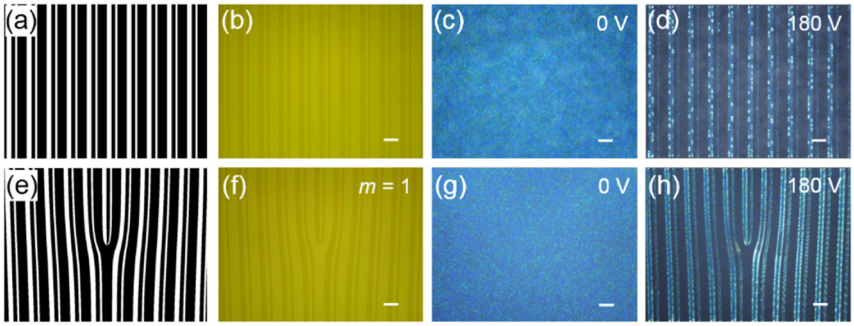

Fig. 1. Phase structures of (a) DG and (e) DVG, where black for 0 and white for π. Micrographs of (b) DG and (f) DVG patterned electrodes. Micrographs of PSBPLC cells at (c), (g) voltage-off state and (d), (h) voltage-on state with 180 V applied. The scale bars are all 100 μm.

Figures 1(c) and 1(g) present micrographs of the BPLC DG and DVG at voltage-off state. Uniform platelet textures are observed. Due to the wavelength selective Bragg reflection, different color domains exist in different orientated BPLC cubic lattices. As the cubic lattices are optically isotropic and their Kerr effects are independent on orientations, the non-uniform orientation here will not affect the EO properties [33]. After vertical field applied, the

#258583 Received 1 Feb 2016; revised 7 Mar 2016; accepted 7 Mar 2016; published 9 Mar 2016

electrodes covered regions turn darker while uncovered regions remain unchanged, as revealed in Figs. 1(d) and 1(h). The reason is that the LCs tend to reorientate along the electric filed, leading to reduced Bragg reflection. As we can see, the profiles are consistent with the patterned electrodes which is caused by external field induced EO tuning of the BPLC. DG and DVG shaped phase profiles are thus obtained with alternation of isotropic and vertical field induced ordinary refractive indices. In Figs. 1(d) and 1(h), the narrow boundary lines between adjacent regions are induced by the fringe field [34], and will alternate from bright to dark state when rotating the sample under crossed polarizers.

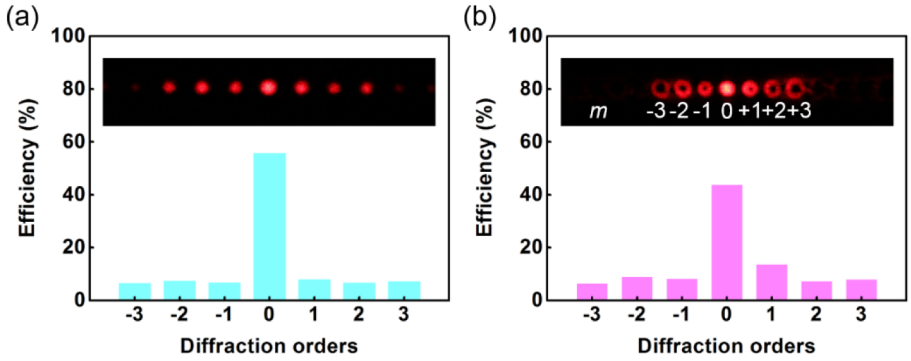

Fig. 2. Light energy distribution in the 1 × 7 diffraction orders of (a) DG and (b) DVG. The insets are corresponding photos of diffraction patterns with 180 V applied.

In our experiment, a 632.8 nm laser beam passes first through a polarizer and then a half-wave plate to generate a linearly polarized light. Afterwards, it normally incidents to the sample and the diffracted orders are received by a photodetector. At 0 V, only a Gaussian beam is observed (as the inset in Fig. 3) since the BPLC is optical isotropic, and the cell works as a uniform dielectric film. Figure 2(a) presents the energy distribution of the DG sample with a voltage of 180 V applied, with corresponding diffraction pattern shown in the inset. The energy distribution and diffraction pattern of BPLC DVG are shown in Fig. 2(b). Due to the forked dislocation, the diffraction orders turn to OVs with topological charges given by *nm*. When altering the incident polarization, no obvious difference is observed, indicating a good polarization independence. The reason is that the phase profiles are generated through the phase difference between n_i and $n_o(E)$, both of which are independent on the polarization of normally incident laser beams [34]. Unfortunately, it can be seen here that the energy distribution of each diffraction order is not so uniform and the energy of the 0th order is still high. The nonuniformity is mainly caused by the preparation error in fabricating the patterned electrodes and the fringe field effect. The phase difference Γ between adjacent regions does not reach π, making the 0th order higher than other orders. This can be improved by optimizing the geometric parameters of the cell gap, or by introducing BPLC with larger Kerr constant and birefringence.

#258583 Received 1 Feb 2016; revised 7 Mar 2016; accepted 7 Mar 2016; published 9 Mar 2016

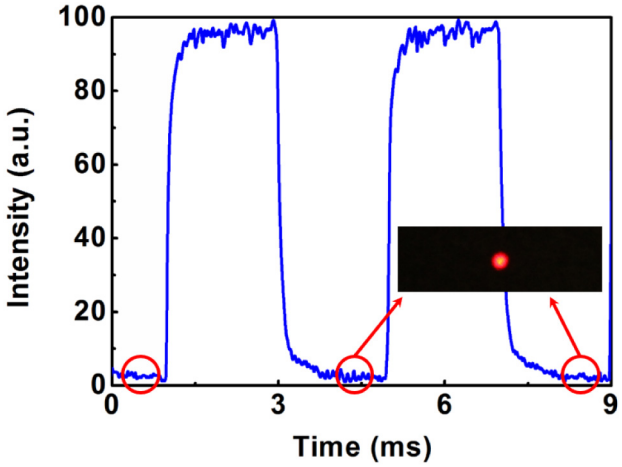

Fig. 3. EO response of the BPLC DVG. The voltage-off state is shown as inset.

A switch between on and off states could be easily accomplished for the DG and DVG via voltage control. The EO response of the BPLC DVG is tested. The switching on/off time here is defined as the duration that the intensity of the 1st order optical vortex changes from 10% to 90% and reverse. As shown in Fig. 3, the measured switching on and off alternating between 0 V and 180 V are τ_{on} = 545 μs and τ_{off} = 673 μs respectively, both of which are in sub-millisecond scale.

4. Conclusion

In this work, optical array generators based on BPLC DG and DVG are demonstrated. The phase profile is formed by the alternation of n_i and $n_o(E)$ induced by vertical field. The devices can convert Gaussian beams to Gaussian beam array or vortex beam array with equal-energy distribution. They exhibit merits of fast response and polarization independence. This approach supplies a new strategy for optical array generator, providing great potentials in array illumination, beam shaping and optical communications.

Acknowledgments

This work was sponsored by the National Natural Science Foundation of China (NSFC) programs (Nos. 11304151, 61490714, 61435008 and 61575093).

#258583 Received 1 Feb 2016; revised 7 Mar 2016; accepted 7 Mar 2016; published 9 Mar 2016